Skin Research and Technology 2005: 11: 36–41
Printed in Denmark · All rights reserved

Skin Research and Technology

Colors in atypical nevi: a computer description reproducing clinical assessment

Stefania Seidenari[1], Giovanni Pellacani[1] and Costantino Grana[2]

[1]*Department of Dermatology, and* [2]*Department of Computer Engineering, University of Modena and Reggio Emila, Italy*

Background/purpose: Atypical nevi (AN) share some dermoscopic features with early melanoma (MM), and computer elaboration of digital images could represent a useful support to diagnosis to assess automatically colors in AN, and to compare the data with those referring to clearly benign nevi (BN) and MMs.

Methods: An image analysis program enabling the numerical description of color areas in melanocytic lesions was used on 459 videomicroscopic images, referring to 76 AN, 288 clearly BN and 95 MMs.

Results: Black, white and blue-gray were more frequently found in AN than in clearly BN, but less frequently than in MMs. Color area values significantly differed between the three groups.

Conclusion: The clinical–morphological interpretation of the numerical data, based on the mathematical description of the aspect and distribution of different color areas in different lesion types may contribute to the characterization of AN and their distinction from MMs.

Key words: melanoma – epiluminescence microscopy – dermoscopy – image analysis – automated diagnosis

Accepted for publication 13 May 2004

SURFACE MICROSCOPY, which uses incident light magnification systems associated to the epiluminescence technique or polarized light, improves diagnostic accuracy for melanoma (MM), especially for difficult-to-diagnose lesions (1–3). To overcome Unavoidable subjectivity and variability in the interpretation of dermoscopic images (4), programs for image analysis have been recently developed that enable the numerical description of the morphology of pigmented skin lesion images. Some of them have been shown to provide a reproducible quantification of lesion features and an aid to clinical diagnosis (5–13). Automated image assessment is based on a new mathematical semiology, defining the geometry, the texture, the pigmentation and the colors of the lesion. The assessment of colors represents an essential step in MM diagnosis, both when performing pattern analysis on dermoscopic images and when using semi-quantitative methods (14–20). Malignant lesions frequently show more than three colors, whereas in nevi, three or less than three colors are usually observed (19). Moreover, different colors prevail in different lesion types.

Recently, we described an image analysis method for the evaluation of colors in melanocytic lesion (ML) images based on an approach that shares some similarities with the human perception of colors (20). using this automated evaluation method, we were able to show that black, white and blue-gray are more frequently found in MMs than in nevi, and that the former show a higher number of colors than the latter, pointing to the crucial diagnostic importance of color parameters.

Atypical nevi (AN) share some dermoscopic features with early MM, and a correct diagnosis cannot be always established on a clinical or on a dermoscopic basis. In these cases, however, the choice between no therapeutic intervention and excision is crucial, and computer image elaboration could represent a fundamental support to clinical diagnosis.

The aim of this study was to assess automatically colors in images referring to AN, and to compare the data with those referring to clearly benign nevi (BN) and MMs. A mathematical description of the aspect and distribution of different color areas in different lesion types is provided, and a clinico-morphological interpretation of the numerical data is presented.

Materials and Methods

Image database

Four hundred and fifty-nine ML images, referring to 76 AN, 288 clearly BN and 95 MMs were studied.

The images were retrospectively subdivided into three groups according to clinical, dermoscopic and histopathologic criteria. Two hundred and eighty-eight of these images corresponded to lesions with a clearly benign aspect (BN) and only 30% of these were excised and examined. On non-excised lesions, a 6-month follow-up was performed. The second group (AN) included 76 lesions with atypical dermoscopic aspects and negative histopathology for MM. The third group (MMs) comprised 95 lesions with atypical dermoscopic aspects and histopathologic diagnosis of MM (mean thickness = 0.6 ± 0.7).

Image acquisition system

Images were acquired by means of a digital videomicroscope (VideoCap 200, DS-Medica, Milan, Italy), with a 20-fold magnification, enabling the lesion to be fully visualized. The instrument has been described elsewhere (9, 11). The images were digitized by means of a Matrox Orion frameboard and stored by an image acquisition program (VideoCap 8.09, DS-Medica, Milan, Italy), which runs under Microsoft Windows. The digitized images offer a spatial resolution of 768×576 pixels and a resolution of 16 million colors.

Image analysis program

The image analysis program was created using MS visual C++ 6.0 both for palette generation and color region detection and elaboration.

Interactive creation of the color palette

Our palette was created using a database comprising 30 PSL images unequivocally showing black, dark brown, light brown, red, white and blue-gray color components. The palette's six color groups are made up of 98 color patches, corresponding to the minimum number of color shades permitting a sufficiently accurate description of single colors.

Color region detection

The obtained palette was used to extract the color regions from the images. Each pixel of the image was assigned to the color patch that minimizes its Euclidean distance in the RGB color space. After assigning all pixels to their corresponding patches, those belonging to the same group were merged together to form the region corresponding to that particular color. The method for palette creation and color region detection has already been described in detail (20, 21).

Color region parameters

For each color region, a set of parameters was extracted, in order to describe the color region properties numerically.

After detection of the lesion border (22) and extraction of reference geometrical measures, such as centroid and main inertia axes, according to standard algorithms, the lesion was divided into two zones corresponding to different semantic parts (Fig. 1). The internal zone corresponds to 80% of the distance between the centroid and the furthest border point along the same direction. The remaining part of the lesion belongs to the external zone. For each color region, measurements were made of the area, distance from the barycenter, spread, color area distribution in the internal and the external part of the lesion and asymmetries. The mathematical and clinical meaning of these parameters are illustrated in Table 1.

Statistics

For statistical analysis, the Statistical Package for Social Sciences (SPSS) (release 10.0.06, 1999; SPSS Inc., Chicago, IL, USA.) was used. As basic statistics, mean and standard deviation of color parameters were calculated for AN, BN and MMs. Differences between values referring to the three groups were evaluated using the Mann–Whitney *U*-test for independent samples. As regards the

TABLE 1. List of parameters and their clinical meaning

Parameter abbreviation	Range	Parameter description	Parameter meaning
AREA	(0–1)	Percentage of the color area in respect of the lesion area	Extension of the color area
DIST-BAR	(0–1)	Distance between color area barycenter and lesion barycenter	Color distribution balance
SPRE	(1–∞)	Mean of the square distance of the color area pixels from the barycenter	Color region density
PERC-INT	(0–1)	Percentage of the color area in the internal zone	Color distribution
PERC-EXT	(0–1)	Percentage of the color area in the external zone	Color distribution
ASYM-MAX	(0–1)	Maximum asymmetry along major or minor axis	Asymmetry of the color distribution
ASYM-MIN	(0–1)	Minimum asymmetry along major or minor axis	Asymmetry of the color distribution
%	(0–100)	Presence/absence	Percentage of lesions presenting the color area

frequency of single colors, differences between different ML values were evaluated using the χ^2 test. A P-value <0.01 was considered significant.

Results

Mean and standard deviation of the parameters calculated for each color group are listed in Table 2.

In AN, black color areas were detected more frequently than in BN, and less frequently than in MMs (AN, 79%; BN, 52%; MMs, 87%). Black areas were larger in MMs with respect both to AN and to BN, whereas, differences referring to area size between AN and BN were not significant. In AN, the imbalance (distance from the barycenter) and asymmetry of black areas were less pronounced than in MMs. Black areas were located in the external zone by an extent of 10.8% of MMs, and 2.9% in AN. In benign lesions, the external zone appeared only minimally involved, containing only 1.5% of black areas.

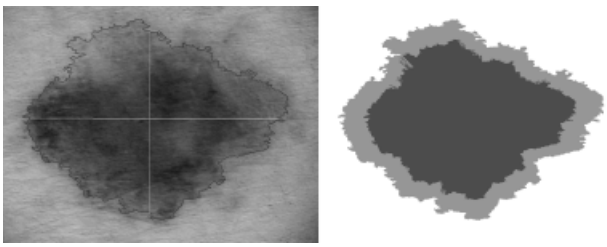

Fig. 1. After detection of the lesion border and extraction of reference geometrical measures, such as centroid and main inertia axes, according to standard algorithms, the lesion is divided into two zones corresponding to different semantic parts. The internal zone corresponds to 80% of the distance between the centroid and the furthest border point along the same direction. The remaining part of the lesion belongs to the external zone.

Most lesions presented dark brown areas (AN, 96%; BN, 95.5%; MMs, 96%). In AN they were larger, more balanced, more compact and more symmetric than in MMs. In nevi, both BN and AN, the dark brown area was distributed predominantly in the internal portion of the lesion, whereas in MMs 27% of it was located in the external zone.

Light brown areas were present in 71% of AN, in 75% of MMs and in 86% of BN. In AN, the distance from the barycenter and asymmetry of light brown areas showed intermediate values between those of BN and MMs.

Red areas were detected in 28% of AN, 26% of BN and 29% of MMs. Red areas were more unbalanced, more compact and more asymmetric in MMs with respect to AN, whereas no differences between the two nevi populations were observed.

White areas were found in 24% of MMs, 9% of AN and 4.5% of BN (Fig. 2). In AN they were

TABLE 2. Color parameters in atypical nevi (AN), clearly benign nevi (BN) and melanomas (MMs)

	Area	DistBar	Spread	AsMax	AsMin	Percint	PercExt
Black							
BN	0.232 ± 0.181	0.049 ± 0.035	0.683 ± 1.139	0.282 ± 0.224	0.118 ± 0.137	0.985 ± 0.046	0.015 ± 0.046
AN	0.294 ± 0.226	0.057 ± 0.049	0.618 ± 0.756	0.31 ± 0.254	0.116 ± 0.145	0.971 ± 0.036*	0.029 ± 0.036*
MM	0.377 ± 0.242*,†	0.087 ± 0.073*,†	0.652 ± 1.03	0.37 ± 0.288*	0.152 ± 0.178	0.892 ± 0.083*,†	0.108 ± 0.083*,†
Dark brown							
BN	0.317 ± 0.155	0.042 ± 0.041	0.668 ± 1.067	0.193 ± 0.185	0.081 ± 0.112	0.92 ± 0.112	0.08 ± 0.112
AN	0.327 ± 0.162	0.055 ± 0.056	0.938 ± 1.712	0.229 ± 0.21	0.079 ± 0.102	0.839 ± 0.16*	0.161 ± 0.16*
MM	0.239 ± 0.14*,†	0.101 ± 0.076*,†	1.109 ± 1.091*,†	0.377 ± 0.26*,†	0.154 ± 0.161*,†	0.73 ± 0.172*,†	0.27 ± 0.172*,†
Light brown							
BN	0.283 ± 0.191	0.052 ± 0.049	1.568 ± 2.154	0.205 ± 0.17	0.08 ± 0.086	0.748 ± 0.192	0.252 ± 0.192
AN	0.211 ± 0.153*	0.078 ± 0.067*	2.404 ± 3.364*	0.278 ± 0.201*	0.134 ± 0.142*	0.65 ± 0.182*	0.35 ± 0.182*
MM	0.238 ± 0.175	0.13 ± 0.1*,†	1.969 ± 2.513*	0.446 ± 0.292*,†	0.191 ± 0.21*	0.631 ± 0.178*	0.369 ± 0.178*
Red							
BN	0.071 ± 0.066	0.069 ± 0.052	5.749 ± 2.661	0.271 ± 0.177	0.109 ± 0.112	0.773 ± 0.161	0.227 ± 0.161
AN	0.055 ± 0.065	0.081 ± 0.057	5.858 ± 2.362	0.311 ± 0.221	0.122 ± 0.104	0.741 ± 0.159	0.259 ± 0.159
MM	0.07 ± 0.049†	0.142 ± 0.073*,†	3.456 ± 2.196*,†	0.521 ± 0.269*,†	0.216 ± 0.165*,†	0.766 ± 0.123	0.234 ± 0.123
White							
BN	0.06 ± 0.047	0.078 ± 0.054	5.038 ± 3.133	0.292 ± 0.193	0.132 ± 0.161	0.539 ± 0.193	0.461 ± 0.193
AN	0.092 ± 0.102	0.114 ± 0.078	3.816 ± 2.978*	0.504 ± 0.337	0.204 ± 0.284	0.687 ± 0.244	0.313 ± 0.244
MM	0.130 ± 0.044*,†	0.163 ± 0.086*	3.8 ± 2.684*	0.626 ± 0.282*	0.23 ± 0.239	0.759 ± 0.153*	0.241 ± 0.153*
Blue-gray							
BN	0.042 ± 0.017	0.032 ± 0.017	3.161 ± 1.382	0.142 ± 0.094	0.048 ± 0.045	0.89 ± 0.055	0.11 ± 0.055
AN	0.041 ± 0.008	0.048 ± 0.043	3.352 ± 0.933	0.203 ± 0.123	0.099 ± 0.081	0.854 ± 0.095	0.146 ± 0.095
MM	0.052 ± 0.036	0.08 ± 0.054*	3.844 ± 2.01	0.304 ± 0.194	0.15 ± 0.143	0.794 ± 0.14	0.206 ± 0.14*

*Statistically significant in respect to clearly benign lesions.
†Statistically significant in respect to atypical lesions.

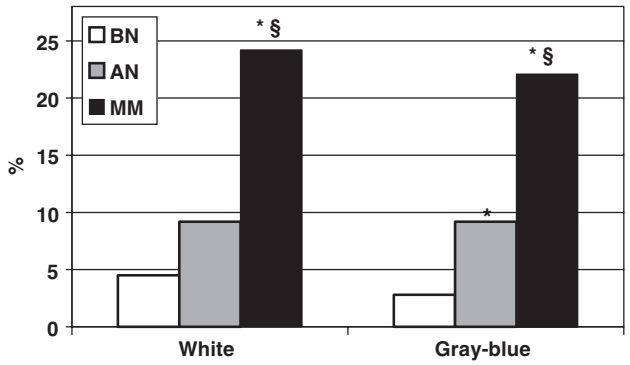

*Fig. 2. Frequency of the presence of white and gray-blue areas in atypical nevi, clearly benign nevi and melanomas. *Statistically significant with respect to clearly benign lesions; §statistically significant with respect to atypical lesions ($P < 0.01$).*

larger than in BN, but smaller than in MMs. In the latter, white areas were more unbalanced, more compact, more asymmetric and more localized in the inner part of the lesion with respect to nevi.

In AN, blue-gray areas were more frequently detected with respect to BN, but less frequently than in MMs (AN, 9%; BN, 3%; MMs, 22%) (Fig. 2). In AN blue-gray areas were less balanced and less symmetric with respect to BN, but smaller, more balanced, more compact and more symmetric with respect to MMs. A significantly higher percentage of the blue-gray area was located in the external zone in MMs with respect to nevi, whereas no differences were observed between AN and BN.

Discussion

The clinical significance of AN is still a matter of controversy. Some authors consider AN as potential MM precursors (23), while others believe that they indicate an increased risk of developing MM (24, 25). Anyhow, the clinical criteria attributed to AN overlap qualitatively with those traditionally used for the diagnosis of MM. These include asymmetry, border irregularity, pigment variegation, uneven surface topography and large size. From a dermoscopic point of view, AN span a continuum from minimally abnormal nevi to markedly abnormal nevi that cannot be distinguished from a malignant lesion and must be excised to rule out MM. Therefore, to avoid unnecessary excisions, the characterization and the identification of AN are of utmost importance.

Color identification is crucial for the diagnosis of pigmented skin lesions by means of epiluminescence microscopy. The colors of the lesions are usually described by means of six main color groups: black, dark brown, light brown, red, white and blue-gray. Some colors and hues are of greater clinical relevance than others: gray, blue, pink, white and black areas are suggestive of MM. Moreover, malignant lesions frequently show more than three colors, whereas in nevi, three or less than three colors are usually observed (19). In semi-quantitative methods, colors contribute substantially to the final score (15, 18). In the study by Salopek et al. (26), the presence of seven colors, their predominance and the total number of colors seen in images referring to MMs and AN was assessed. The authors observed that the presence of red, blue, gray and white was a statistically significant predictor of MM, as was the presence of four or more colors. Blue and white were highly specific features, whereas more than three colors was the only sensitive parameter for early MM. According to Nilles et al. (27), 100% of MMs exhibit more than three colors, whereas only 87% of AN do so. AN were classified according to the distribution and intensity of their pigmentation by Hoffmann-Wellenhof et al. (28). Central and peripherical hyper- or hypopigmentation, arranged in a localized and multifocal distribution, was considered. The authors draw attention to the peripherically hyper-pigmented type, mimicking an *in situ* MM. Kittler et al. (29), who used digital ELM for the follow-up of patients with multiple AN, considered color changes to be substantial modifications, therefore indicating a possible transformation into MM.

The aim of this study was to describe colors in AN, and to compare the data with those referring to BN and to MMs. For this purpose we used an image analysis program enabling the numerical description of the morphology of ML images, recently developed by us (20, 21), based on an approach that is similar to the human perception of colors. A color palette comprising six color groups (black, dark brown, light brown, gray-blue, red and white) was interactively created by selecting single color components inside ML images acquired by means of a digital videomicroscope, and was integrated in the image analysis program. In a previous study ,colors were assessed by the computer on nevi and MMs, and the results were compared with the evaluation of lesion colors performed by clinicians, demonstrating a high correlation between the identification process of colors by trained dermatologists and the new computer program (20). By this

method we showed that some colors are more frequently found in MMs than in nevi, and that MM images present a higher number of colors than images of nevi. Furthermore, the numerical description of color area extension and distribution by means of automatically extracted parameters enabled the distinction of malignant vs. benign MLs (21). In this study we showed that black, white and blue-gray are more frequently found in AN with respect to BN, but less frequently than in MMs. Moreover, a description of the distribution of color areas in AN was provided by mathematical parameters.

If we consider AN as possible MM precursors, we could imagine a continuous transformation process leading from the aspect of a clearly benign nevus to the aspect of MM (Fig. 3). Numerical data can be translated into a suitable clinical description, and color type and distribution in MLs can be described in a ''dynamic'' way. Starting from the ML with an obvious benign dermoscopic aspect, where dark color areas (dark brown and black) of small size are symmetrically distributed in or around the center, we can observe a progressive migration of these color regions towards the periphery, where they become larger and more unbalanced and asymmetric. The extension of red does not vary between the three ML populations; however, its distribution progressively changes from BN to MMs. This is expressed by an advancing imbalance of red areas, which appear more asymmetric in AN and MMs. In the latter population the red color component is more localized, possibly corresponding to areas of increased vascularization. The extent and the distribution of white progressively change from BN to MMs, showing an intermediate aspect in AN. While in BN the white color component is scarce and is part of the nevus texture, being distributed all over the image, intermingled with other colors and arranged symmetrically, in MMs white areas become larger, less balanced and less symmetric, more compact and located in the inner part of the lesion, possibly corresponding to regression areas. The blue-gray color component progressively increases from BN to MMs, and it becomes unbalanced, asymmetric and more located in the external part of the lesion in MMs, indicating the presence of asymmetrically distributed gray–blue areas in malignant lesions.

The parameters used by programs for image analysis usually derive from mathematical definitions not easily intelligible to clinicians and they do not correspond to the human perception of characteristic clinical aspects. Our system not only resolves the image into color areas according to the usually used clinical examination process but also supplies a description of their extension and distribution.

The reproducibility of color assessment is generally high, pointing to the high diagnostic relevance of color parameters. In a recent consensus study on dermoscopy via the internet, intra-observer agreement showed a *k*-value of 0.64 for the number of colors in the ABCD rule, and of 1 for the presence of a single color according to Menzies [4]. Reproducibility of color evaluation is high even in images of low quality, and colors are less affected by compression than morphological details in the image. This was shown by a study assessing the informativeness of compressed videomicroscopic images (30), where differences between κ values of uncompressed and compressed images referring to intra-observer agreement on colors were higher than for other features. This indicates the potential of computer-aided color assessment-based diagnosis in an era where teledermatology is going to become increasingly important.

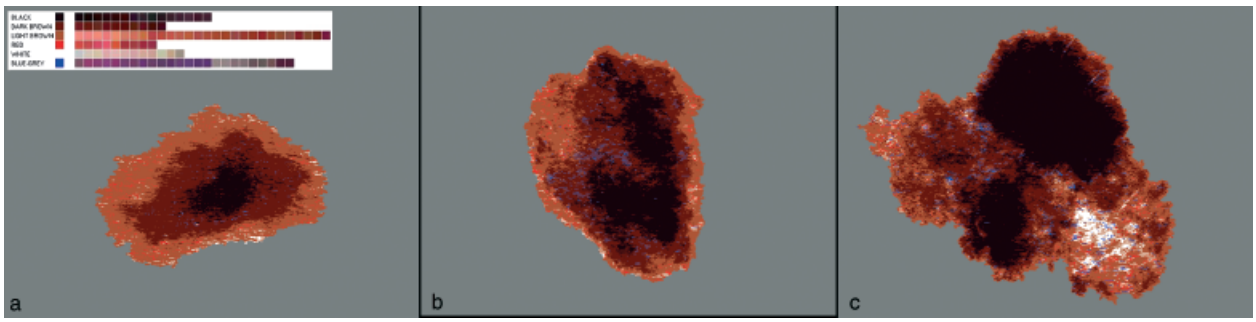

Fig. 3. Reconstruction of colors (pseudo-colors) (a) in clearly benign nevi, (b) in atypical nevi and (c) in melanomas, according to the numerical description of color areas by the computer. The color palette is represented in the inset.

Acknowledgements

This study was partially supported by Ministero dell'Istruzione dell'Università e della Ricerca, grant number 2001068929. The authors have no conflict of interest to disclose. The contents of the manuscript have not been previously published and have not been submitted elsewhere.

References

1. Pehamberger H, Steiner A, Wolff K. In vivo epiluminescence microscopy of pigmented skin lesions. I. Pattern analysis of pigmented skin lesions. J Am Acad Dermatol 1987; 17: 571–583.
2. Kenet RO, Kang S, Kenet BJ, Fitzpatrick TB, Sober AJ, Barnhill RL. Clinical diagnosis of pigmented lesions using digital epiluminescence microscopy. Arch Dermatol 1993; 129: 157–174.
3. Bahmer FA, Fritsch P, Kreusch J et al. Terminology in surface microscopy. J Am Acad Dermatol 1990; 23: 1159–1162.
4. Argenziano G, Soyer HP, Chimenti S et al. Dermoscopy of pigmented skin lesions: results of a consensus meeting via the internet. J Am Acad Dermatol 2003; 48: 679–693.
5. Cascinelli N, Ferrario M, Bufalino R et al. Results obtained by using a computerized image analysis system designed as an aid to diagnosis of cutaneous melanoma. Melanoma Res 1992; 2: 163–170.
6. Green AC, Martin NG, Pfitzner J, O'Rourke M, Knight N. Computer image analysis in the diagnosis of melanoma. J Am Acad Dermatol 1994; 31: 958–964.
7. Hall PN, Claridge E, Morris Smith JD. Computer screening for early detection of melanoma – is there a future? Br J Dermatol 1995; 132: 325–338.
8. Gutkowicz-Krusin D, Elbaum M, Szwaykowski P, Kopf AW. Can early malignant melanoma be differentiated from atypical melanocytic nevus by in vivo techniques? Part II. Automatic machine vision classification. Skin Res Technol 1997; 3: 15–22.
9. Seidenari S, Pellacani G, Pepe P. Digital videomicroscopy improves diagnostic accuracy for melanoma. J Am Acad Dermatol 1998; 39: 175–181.
10. Binder M, Kittler H, Seeber A, Steiner A, Pehamberger H, Wolff K. Epiluminescence microscopy-based classification of pigmented skin lesions using computerized image analysis and an artificial neural network. Melanoma Res 1998; 8: 261–266.
11. Seidenari S, Pellacani G, Giannetti A. Digital videomicroscopy and image analysis with automatic classification for detection of thin melanomas. Melanoma Res 1999; 9: 163–171.
12. Andreassi L, Perotti R, Rubegni P et al. Digital dermoscopy analysis for the differentiation of atypical nevi and early melanoma. Arch Dermatol 1999; 135: 1459–1465.
13. Pellacani G, Martini M, Seidenari S. Digital videomicroscopy with image analysis and automatic classification as an aid for diagnosis of Spitz nevus. Skin Res Technol 1999; 5: 266–272.
14. Braun RP, Rabinovitz H, Oliviero M, Kopf A, Saurat JH. Pattern analysis: a two-step procedure for the dermoscopic diagnosis of melanoma. Clin Dermatol 2002; 20: 236–239.
15. Nachbar F, Stolz W, Merkle T et al. The ABCD rule of dermatoscopy. J Am Acad Dermatol 1994; 30: 551–559.
16. Menzies SW, Ingvar C, McCarthy WH. A sensitivity and specificity analysis of the surface microscopy features of invasive melanoma. Melanoma Res 1996; 6: 55–62.
17. Argenziano G, Fabbrocini G, Carli P, De Giorgi V, Sammarco E, Delfino M. Epiluminescence microscopy for the diagnosis of doubtful melanocytic skin lesions. Comparison of the ABCD rule of dermoscopy and a new 7-point checklist based on pattern analysis. Arch Dermatol 1998; 134: 1563–1570.
18. Blum A, Rassner G, Garbe C. Modified ABC-point list of dermoscopy: a simplified and highly accurate dermoscopic algorithm for the diagnosis of cutaneous melanocytic lesions. J Am Acad Dermatol 2003; 48: 672–678.
19. Mac Kie RM, Fleming C, Mc Mahon AD, Jarret P. The use of the dermatoscope to identify early melanoma using the three-colour test. Br J Dermatol 2002; 146: 481–484.
20. Seidenari S, Pellicani G, Grana C. Computer description of colours in dermoscopic melanocytic lesion images reproducing clinical assessment. Br J Dermatol 2003; 149: 523–529.
21. Pellacani G, Grana C, Seidenari S. Automated description of colours on surface microscopic images of melanocytic lesions. Melanoma Res 2004; 14: 125–130.
22. Grana C, Pellacani G, Cucchiara R, Seidenari S. A new algorithm for border description of polarized light surface microscopic images of pigmented skin lesions. IEEE Trans Med Imaging 2003; 22: 959–964.
23. Greene MH, Clark WH Jr, Tucker MA, Elder DE, Kraemer KH, Guerry D. Acquired precursors of cutaneous malignant melanoma: the familial dysplastic nevus syndrome. N Engl J Med 1985; 312: 91–97.
24. Albert LS, Rhodes AR, Sober AJ. Dysplastic melanocytic nevi and cutaneous melanoma: markers of increased melanoma risk for affected persons and blood relatives. J Am Acad Dermatol 1990; 22: 69–75.
25. Halpern AC, Guerry D IV, Elder DE et al. Dysplastic nevi as risk markers of sporadic (nonfamilial) melanoma: a case control study. Arch Dermatol 1991; 127: 995–999.
26. Salopek TG, Kopf AW, Stefanato CM, Vossaert K, Silverman M, Yadav S. Differentiation of atypical moles (dysplastic nevi) from early melanomas by dermoscopy. Dermatol Clin 2001; 19: 337–345.
27. Nilles M, Boedeker RH, Schill WB. Surface microscopy of naevi and melanoma: clues to melanoma. Br J Dermatol 1994; 130: 349–355.
28. Hofmann-Wellenhof R, Blum A, Wolf I et al. Dermoscopic classification of atypical melanocytic nevi (Clark nevi). Arch Dermatol 2001; 137: 1575–1580.
29. Kittler H, Pehamberger H, Wolff K, Binder M. Follow-up of melanocytic skin lesions with digital epiluminescence microscopy: patterns of modifications observed in early melanoma, atypical nevi, and common nevi. J Am Acad Dermatol 2000; 43: 467–476.
30. Seidenari S, Pellacani G, Righi E, Di Nardo A. Is JPEG-compression of videomicroscopic images compatible with telediagnosis? Comparison between diagnostic performance and pattern recognition on uncompressed TIFF-images and JPEG-compressed ones. Telemed J E Health 2004; 10: 294–303.

Address:
Stefania Seidenari
Department of Dermatology
University of Modena and Reggio Emilia
41100 Modena
Italy
Tel: +39-(0)59 4222464
Fax: +39-(0)59 4224271
e-mail: seidenari.stefania@unimo.it